



## Kinetics and Thermodynamics of Heavy Metal Adsorption using Activated Carbon Developed from Doum Palm Seeds



Mohammed, Y.<sup>1</sup>, Faruruwa, M. D.<sup>1</sup>, Muhammad, A.<sup>1\*</sup> and Haruna, A. S.<sup>2</sup>

<sup>1</sup>Department of Chemistry, Nigeria Defence Academy, Kaduna.

<sup>2</sup>Department of Science and Technology, Nigeria Defence College, Abuja.

\*Corresponding Author Email: [aminumuhammad@gmail.com](mailto:aminumuhammad@gmail.com)

### ABSTRACT

The increase in human population which prompted the need for the construction of industries has led to indiscriminate discharge of industrial effluent by these industries into our environment. This discharges most times contain heavy metal which adversely affected the ecosystem. This research evaluates the adsorption behaviour of activated carbon prepared from *Hyphaenethebaica* nut shells treated with  $K_2CO_3$  for the treatment of heavy metal contaminated water. The characterization was carried out using FTIR and SEM. The batch adsorption technique was employed and the optimum adsorption was observed at adsorbent dose of 0.6g, initial concentration of 60 ppm, temperature of 60°C. and at contact time of 30 minutes. Optimum adsorption pH for the Heavy Metal adsorption was found to be 2. The adsorption isotherms indicated that the Langmuir isotherm model showed a better correlation ( $R^2 \geq 0.9$ ) for the Heavy Metals compared to Freundlich and Temkin isotherm model. The Pseudo second order adsorption model best described the adsorption kinetics of the Heavy Metals on the adsorbent. The value for the experimental adsorption capacity for  $Cu^{2+}$ ,  $Pb^{2+}$ ,  $Fe^{2+}$  and  $Zn^{2+}$  are 3.83, 4.27, 3.92 and 3.15 respectively corresponded to the calculated adsorption capacity for the pseudo-second-order model for the heavy metals  $Cu^{2+}$ ,  $Pb^{2+}$ ,  $Fe^{2+}$  and  $Zn^{2+}$  calculated as 3.61, 3.71, 2.99 and 2.13 respectively and were closer to the experimental adsorption capacity than the calculated adsorption capacity for the pseudo-first-order model. The correlation coefficient,  $R^2$  values for the pseudo-second-order adsorption model for the heavy metals  $Cu^{2+}$ ,  $Pb^{2+}$ ,  $Fe^{2+}$  and  $Zn^{2+}$  are 0.39, 0.66, 0.51 and 0.33 respectively. The  $\Delta H^\circ$  for the heavy metals  $Cu^{2+}$ ,  $Pb^{2+}$ ,  $Fe^{2+}$  and  $Zn^{2+}$  with positive values of 24.99, 25.09, 24.53 and 25.00 indicates that the adsorption was endothermic and the  $\Delta S$  for the heavy metals  $Cu^{2+}$ ,  $Pb^{2+}$ ,  $Fe^{2+}$  and  $Zn^{2+}$  with values of 79.70, 80.16, 78.66 and 79.79 expresses the affinity of the adsorbent for the heavy metal ions in the adsorbate. The negative values of the  $\Delta G^\circ$  indicated that the adsorption of heavy metal is spontaneous at the temperature under investigation. Thus, activated carbon from  $K_2CO_3$  treated *Hyphaenethebaica* nut shells could therefore be used effectively for the remediation of heavy metals from industrial waste water.

### Keywords:

Kinetics,  
Thermodynamics,  
Isotherm,  
Heavy Metals,  
*Hyphean Thebaica*,  
Doum Palm.

### INTRODUCTION

The increase in human population which prompted the need for the construction of industries has led to indiscriminate discharge of industrial effluent by these industries into our environment. This discharge most times contain heavy metal which adversely affected the ecosystem (Wong *et al.*, 2018). Environmental pollution could be the reason for the shortened life expectancy of human in the world (WHO, 2003). Another point of concern is the carcinogenic nature of some of the heavy metals contained in most of these industrial effluents

(Saminuet *et al.*, 2021). Textile industries are characterized by discharge of large quantities of waste water which contains harmful chemicals due to the raw materials and processes used in the manufacture of finished products (Yusuff, 2004).

Activated carbons are porous materials which are carbonaceous and are categorized by its applications due to unique characteristics in various activities such as treatment and desalination of water, wastewater and air purification (Samsuriet *et al.*, 2014; Koshelevaet *et al.*, 2019; Yousefet *et al.*, 2019). It is an adsorbent material with high

degree of porosity and surface area (Samsuri et al. 2014; Gopinath and Kadirvelu 2018; Morin-Criniet al., 2019). Most activated carbon structures are made up of functional groups such as phenols, lactones which are responsible for the adsorption of contaminants. Also found in the structures are, oxygen, hydrogen, sulphur and nitrogen which are present as functional groups or chemical atoms. The activation processes, type of precursor and thermal purification are fundamental in determining the functional groups which the adsorption properties of the activated carbon depend on (Bhatnagaret al., 2013; Yousefet al., 2019).

The complex nature of activated carbon products makes it difficult to be classified on the basis of their behaviors, surface characteristics and other fundamental criteria. However, activated carbons are given a broad classification for general purposes based on their sizes, preparation methods, and industrial application as; i. Powdered activated carbon (PAC) ii. Granular activated carbon (GAC) iii. Extruded activated carbon (EAC) (Chadaet al., 2012).

Powdered activated carbon (PAC) are made in a particular form as powders or as fine granules with particle size less than 1.00 mm and an average diameter between 0.15 mm and 0.25 mm. Powdered activated carbon present a large surface to volume ratio with a small diffusion distance. These classes of activated carbon are categorized by its carbon particle being retained on 50-mesh sieves usually 0.297 mm (Chadaet al., 2012).

Granular activated carbon (GAC) has a comparatively larger particle size compared to powdered activated

carbon. Thus, granular activated carbon has smaller external surface area and the diffusion of the adsorbate is an important factor. These types of activated carbons are best suited for adsorption of most gases and different vapors because they tend to dissolve rapidly. Granular activated carbons are also used in the treatment of water, de-odorization and are also used in rapid mix basins (Chadaet al., 2012).

Extruded activated carbon (EAC) is combined with powdered activated carbon using a binder and subsequently fused together then extruded into a cylindrical shaped activated carbon block which has a diameter ranging from 0.8mm to 130mm. Due to the low pressure drop experienced and the elevated mechanical strength and low dust content extruded activated carbon are used mainly in gas phase applications (Chadaet al., 2012).

Doum palm fruits (*Hyphaenethebaica*) are desert palm tree which have edible oval fruit. The fruits are originally found in the Nile Valley and are also cultivated very well in the northern part of Nigeria. Doum palm belongs to the palm family, Arecaceae. As displayed in figure 1, the tree has a very unique appearance often each branch divides again in a y form. Doum palm fruit is also a source of potent antioxidants (Hsu et al., 2006). The trunk of a doum palm is dichotomous and is also one of the most important useful plants in the world. Also, roots, stems and leaves of the palm fruit are used in medicine, ropes and baskets (Orwaet al., 2009).



Figure 1: Doum palm fruit (*Hyphaenethebaica*)

## MATERIALS AND METHODS

### Sampling and Sample Pretreatment

The doum palm fruit were collected from the doum palm trees in Yusuf Dantsoho Memorial Hospital, Kaduna.

### Description of sample

Doum palm are smooth and rectangular with rounded edges, shiny brown when ripe. Its fresh weight is about 120g and dry weight is about 60g and each one containing a single seed.

Doum palm also called goruba in northern part of Nigeria have a large hairy seed in its middle which are edible with a shiny orange-brown colour, chewy bitter-sweet taste; very tough that to eat it one must have very strong healthy teeth and gums. The part used in the research is the hard nut shell right underneath the edible part of the doum palm fruit.

### Identification and authentication

The doum palm fruits were taken to the Department of Biological Science Herbarium of Nigerian Defence Academy for proper identification and authentication. After identification and authentication, reference number NDA/BIOH/2023/02 was issued.

### Pretreatment and packaging

Primarily, doum palm fruits were scraped to reveal the doum palm nut shells and then washed to remove husk and dirt from the surface and dried in the oven for four hours at 105 °C. The dried doum palm nut shells were ground and segregated to granular mesh size (2 mm) (Tan *et al.*, 2007).

### Preparation of precursor

Exactly 200g of the pretreated doum palm nut shells was weighed and transferred into a beaker and mixed with the 67g of the activating agent ( $K_2CO_3$ ) in the ratio of 1:3 of activating agent against pretreated doum palm nut shell. Subsequently, 1000cm<sup>3</sup> deionised water was added to dissolve the activating agent in the mixture, followed by drying overnight and further thermal treatment in the oven at 200 °C for 2 h and then stored in an air tight container (Tan *et al.*, 2007).

### Carbonization

The prepared precursor was put into the furnace and thermal treated at 500°C for 3 hours. The resulting materials was cooled and washed with hot deionised water until the pH of the filtrate was nearly 7. The activated carbon thus obtained was finally smoothened, stored in an air tight container and properly labeled for next level of experimental investigations (Tan *et al.*, 2007).

### Adsorbent characterization

The activated carbon was characterized using SEM and FTIR.

### Preparation of Reagents

The multi-element heavy metal solution (1000mg/l) was prepared by diluting 0.25g copper sulphate pentahydrate ( $CuSO_4 \cdot 5H_2O$ ), 1.60g of lead nitrate  $Pb(NO_3)_2$ , 1.24g zinc oxide in 25ml 6N HCl and 6.67g of ferrous ammonium sulfate hexahydrate  $(NH_4)_2Fe(SO_4)_2 \cdot 6H_2O$  in 100ml of distilled water in a 1000 ml volumetric flask and then made up to the mark.

A 100mg/l solution was prepared from the multi-element heavy metal solution by measuring 100ml of the previously prepared 1000mg/l multi-element heavy metal solution in a 1000ml volumetric flask and filling to the mark with distilled water. The solution was then labeled accordingly for further experiment.

### Adsorption Experiment

Batch experiments were performed on magnetic stirrer at 30°C to investigate the effect of adsorbent dosage, contact time, pH, initial concentration and temperature on adsorption of heavy metal ( $Cu^{2+}$ ,  $Fe^{2+}$ ,  $Zn^{2+}$  and  $Pb^{2+}$ ) over the activated carbon.

**Effect of adsorbent dosage:** Exactly 50ml of 100mg/l multi-element solution was measured into a cleaned 250ml conical flask and 0.2g of the adsorbent was added and corked. The solution was stirred using a magnetic stirrer for 30min at 150 rotations per minute (rpm). The solution was then filtered and the filtrate analyzed using AAS for the metal ions. The experiment was repeated for 0.4, 0.6, 0.8 and 1.0g of the adsorbent (Onyeji & Aboje 2011).

**Effect of contact time:** Exactly 50ml of 100mg/l multi-element solution was measured into a cleaned 250ml conical flask and 0.6g of the adsorbent was added and corked. The solution was stirred using a magnetic stirrer for 20min at 150 rotations per minute (rpm). The solution was then filtered and the filtrate analyzed using AAS for the metal ions. The experiment was repeated for 30, 40, 50 and 60 minutes of contact time between the adsorbate and adsorbent (Ekpete *et al.*, 2010).

**Effect of pH:** Exactly 50ml of 100mg/l multi-element solution was measured into a cleaned 250 ml conical flask and pH of the adsorbate adjusted to pH 2 using 0.1M HCl and 0.6g of the adsorbent was then added and corked. The solution was stirred on a magnetic stirrer for 30min at 150 rotations per minute (rpm). The solution was then filtered and the filtrate analyzed using AAS for the metal ions. The experiment was repeated over a pH range of 4 and 6 (Onyeji & Aboje, 2011).

**Effect of temperature:** The effect of temperature/thermodynamics was studied for the prepared heavy metal solutions by varying the temperature at which the reaction takes place at optimized conditions of adsorbent dose, contact time and pH. The temperatures of interest are: 40°C, 50°C and 60°C. Exactly 50ml of the mixtures of adsorbate and adsorbent

were kept in 250ml conical flasks and stirred on a magnetic stirrer at 150rpm. The mixtures were filtered immediately using Whatman filter paper. The filtrates were then analyzed for heavy metals using AAS. Thus, the optimum temperature was determined (Ektepe *et al.*, 2010).

**Effect of initial concentration:** To investigate the effect of concentration, 20mg/l from the 100mg/l heavy metal solution was prepared by transferring 5ml of the heavy metal solution into a 100ml volumetric flask and made up to the mark using distilled water and 0.6g of the adsorbent was added to 50ml of the solution and the pH adjusted using 0.1M HCl to 2. The mixture was then corked and stirred on a magnetic stirrer for 30min at a speed of 150rpm at room temperature. This procedure was repeated for 40mg/l and 60mg/l respectively. The Whatman filter paper was used to filter the mixture and the filtrate analyzed using AAS (Onyeji & Aboje, 2011).

#### Adsorption isotherm studies

Adsorption isotherms for the remediation of heavy metals were investigated for 20, 40 and 60 mg/l initial metal ion concentrations using optimum conditions of adsorbent dose, contact time, pH and temperature and stirred on a magnetic stirrer at 150 rotation per minute (rpm). The solutions were then filtered and the filtrate analyzed using AAS for the metal ions. Three isotherm models, namely Freundlich, Langmuir and Temkin, were employed.

#### Adsorption thermodynamics

Exactly 50ml of the multi-element heavy metal solution in a 250ml conical flask was mixed with 0.6g of the adsorbent under optimum conditions of contact time, initial concentration and pH at temperature of 40°C was stirred on a magnetic stirrer at 150rpm. The mixtures were filtered immediately using Whatman filter paper. The filtrates were then analyzed for heavy metals using AAS for the metal ions. This procedure was repeated at 50 and 60°C respectively.

#### Adsorption kinetics

Exactly 50ml of the multi-element heavy metal solution in a 250ml conical flask was mixed with 0.6g of the adsorbent under optimum conditions of temperature, initial concentration and pH at a contact time of 20 minutes and was stirred on a magnetic stirrer at 150rpm. The mixtures were filtered immediately using Whatman filter paper. The filtrates were then analyzed for heavy metals using AAS for the metal ions. This procedure was repeated for 30, 40, 50, and 60 minutes respectively.

## RESULTS AND DISCUSSION

### Characterization of the Adsorbent

Surface morphology of the activated carbons was imaged by the use of a Scanning Electron Microscope (SEM) and

then the functional groups present on the activated carbon before and after adsorption was analyzed using Fourier transform infrared spectroscopy (FTIR).

### Scanning electron microscope (SEM)

Scanning Electron Microscope (SEM) of the adsorbent was used to determine the pore structure of the activated carbon and it is displayed in Figure 2 and 3.

The surface structures of precursors were imaged to be rough and uneven. Substantial amount of pore structure exists on the surface with a series of rough cavities being distributed over the surface of adsorbent. This was due to the breakdown at high temperature accompanied by evaporation of the volatile compounds leaving the adsorbent with well-developed pores. During the activation process, the C-K<sub>2</sub>CO<sub>3</sub> reaction rate increased, as thus resulting in the carbon "burn off" which resulted in development of good pores on the adsorbent. The C-K<sub>2</sub>CO<sub>3</sub> reaction also increased the porosity of activated carbon and also resulting in the creation of new pores due to the loss of volatile components and carbon in the form of CO and CO<sub>2</sub> (Auta and Hameed 2011). The physiochemical treatment was effective in producing porous adsorbent thus increasing the surface area.

As seen from Figures 2 and 3, the adsorbent prepared by activating doum palm nutshell with potassium carbonate shows the presence of several micropores structure of different sizes. The images were taken at the magnifications of 5000x and 7000x with an objective lens aperture of 50 μm and 20μm respectively. At this magnificent and field depth, micropores were visible. These pores serve as the active sites, where adsorption of the heavy metals takes place.

### Fourier transform infrared spectroscopy (FTIR)

Fourier transform infrared (FTIR) spectra and absorption bands of K<sub>2</sub>CO<sub>3</sub> impregnated doum palm nut shell activated carbon before and after heavy metal uptake were recorded in the range of 4000-500cm<sup>-1</sup> as depicted in Figure 4 and 5. The spectra showed that the activated carbon retained some functional groups. In the spectrum of the activated carbon before adsorption the characteristic absorption of alkenes (-C=C), ether (C-O) and ethers at 670.9cm<sup>-1</sup>, 1051.1cm<sup>-1</sup> and 1203.9cm<sup>-1</sup> respectively. Other functional groups observed were amines (N-H) and nitriles (C=N) at 1558.0 and 2322.1cm<sup>-1</sup> respectively. The intense peaks at 3906.3cm<sup>-1</sup>, 3649.1cm<sup>-1</sup>, 3589.4cm<sup>-1</sup> and 3354.6cm<sup>-1</sup> are assigned to the stretching vibration of hydroxyl group (O-H) band (Hidayat 2017) (Nurmiyanto *et al.*, 2016).

The spectrum of the activated carbon after adsorption of the heavy metal was characterized by shifts in the position and intensities of bands when compared to the spectrum of the activated carbon before adsorption. This indicates that interactions were established during the heavy metal remediation process. The shift in the band of the hydroxyl

group (O-H) from  $3906.3\text{cm}^{-1}$  in the case of before adsorption to  $3753.4\text{cm}^{-1}$  after adsorption, highlighted the existence of hydrogen bonding by the activated carbon and the heavy metals.

A similar phenomenon was reported by Abel *et al.* (2022) for cadmium ion entrapment process and Mone *et al.*

(2020) for the heavy metal uptake by chitosan grafted adsorbent (Mone *et al.*, 2020). Other shifts in peaks assigned to C-H and C-O groups, after adsorption of heavy metal reveals that the groups are involved in the remediation of heavy metals (Liu *et al.*, 2020).

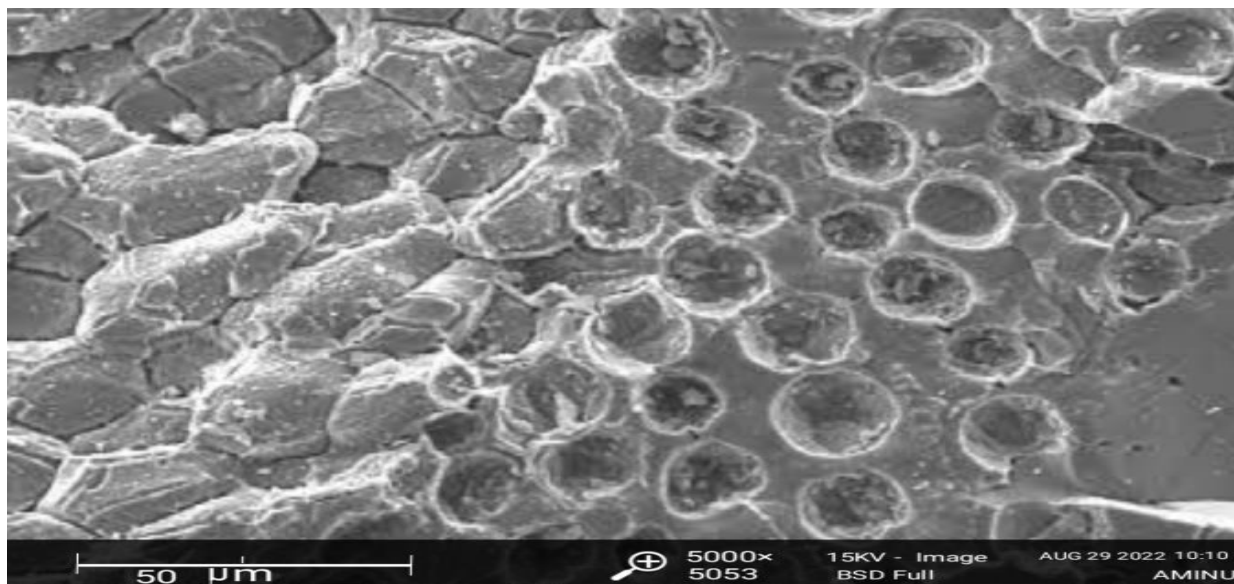


Figure 2: SEM Image of Adsorbent, at X 5000

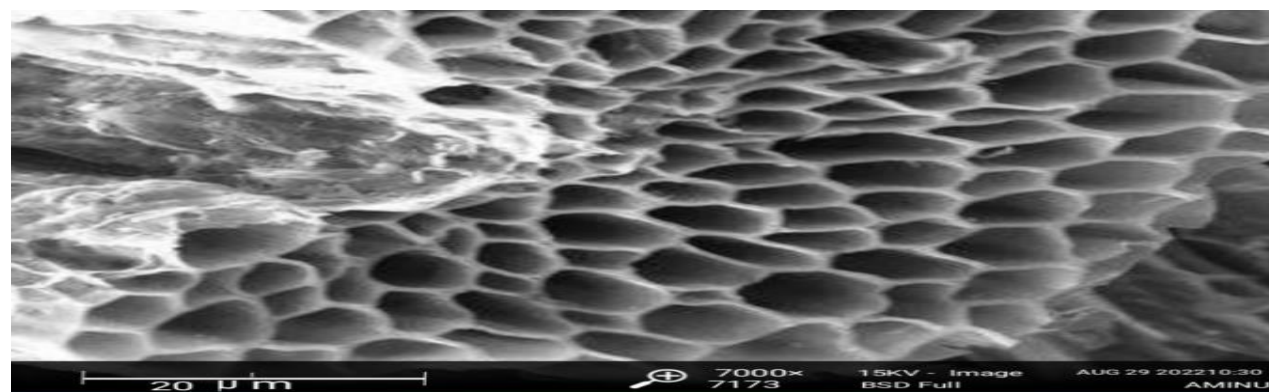


Figure 3: SEM images of adsorbent at X 7000

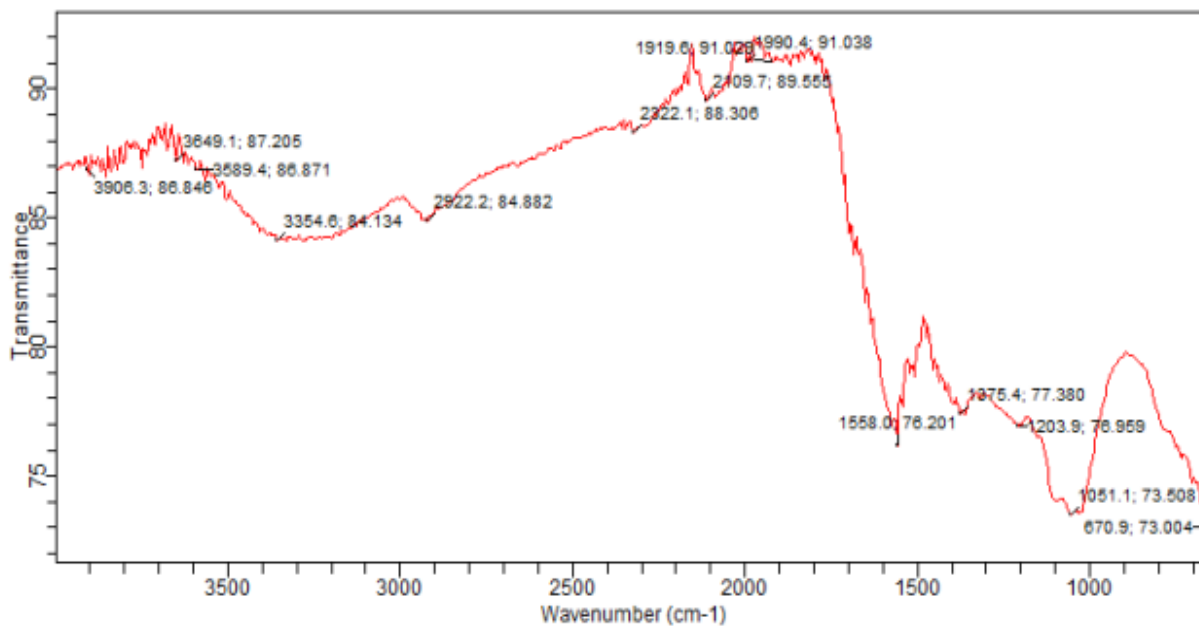


Figure 4: FTIR Spectra for activated carbon before adsorption

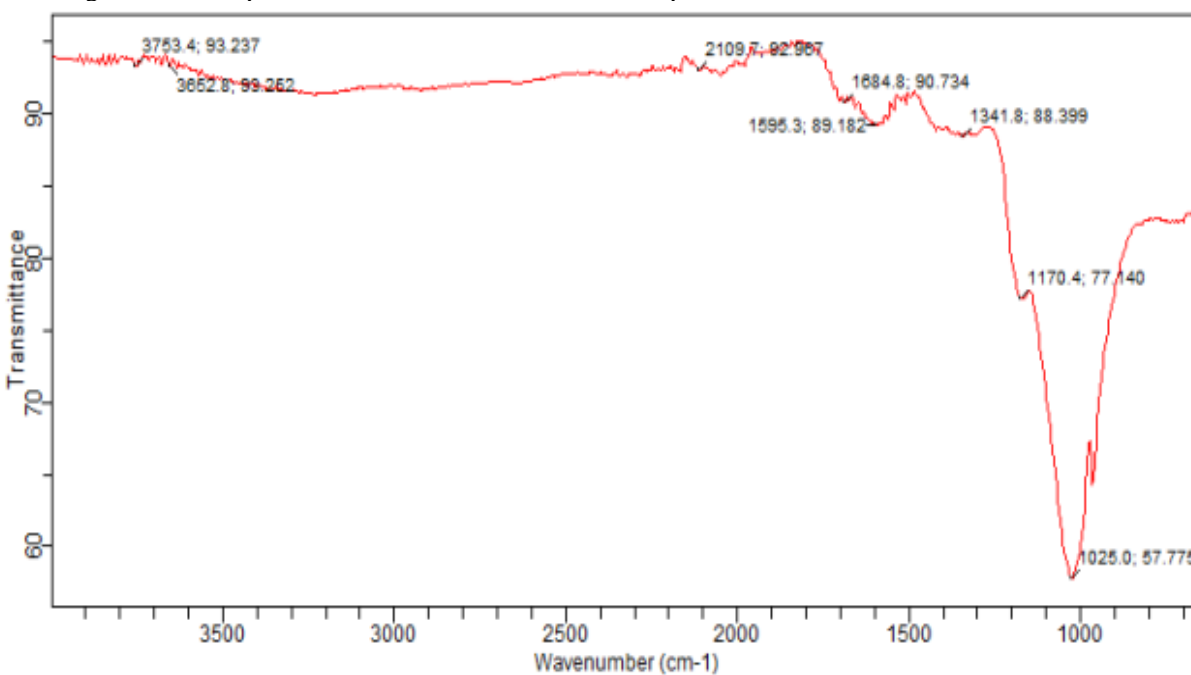


Figure 5: FTIR Spectra for activated carbon after adsorption

**Table 1: Effect of contact time on the remediation of heavy metals**

Time(min)/Cu <sup>2+</sup>	Co mg/l (Cu <sup>2+</sup> )	Ce mg/l	q <sub>e</sub>	%Re
20	100	34.2	5.48	65.8
30	100	5.46	7.88	94.54
40	100	7.67	7.69	92.33
50	100	26.47	6.13	73.53
60	100	17.99	6.83	82.01
Time(min)/Pb <sup>2+</sup>	Co mg/l (Pb <sup>2+</sup> )	Ce mg/l	q <sub>e</sub>	%Re
20	100	24.03	6.33	75.97
30	100	11.67	7.36	88.33

40	100	18.08	6.83	81.92
50	100	38.59	5.12	61.41
60	100	32.15	5.65	67.85
<b>Time(min)/Zn<sup>2+</sup></b>	<b>Co mg/l (Zn<sup>2+</sup>)</b>	<b>Ce mg/l</b>	<b>q<sub>e</sub></b>	<b>%Re</b>
20	100	31.55	5.70	68.45
30	100	4.29	7.98	95.71
40	100	13.89	7.18	86.11
50	100	14.49	7.13	85.51
60	100	19.27	6.73	80.73
<b>Time(min)/Fe<sup>2+</sup></b>	<b>Co mg/l (Fe<sup>2+</sup>)</b>	<b>Ce mg/l</b>	<b>q<sub>e</sub></b>	<b>%Re</b>
20	100	36.72	5.27	63.29
30	100	1.4	8.22	98.60
40	100	3.71	8.02	96.29
50	100	19.01	6.75	80.99
60	100	9.18	7.57	90.82

**Table 2: Effect of adsorbent dose on remediation of heavy metals**

<b>Dose/Cu<sup>2+</sup></b>	<b>C<sub>0</sub> mg/l (Cu<sup>2+</sup>)</b>	<b>C<sub>e</sub> mg/l</b>	<b>q<sub>e</sub></b>	<b>%Re</b>
0.2g	100	39.19	15.20	60.82
0.4g	100	26.2	9.22	73.80
0.6g	100	3.93	8.01	96.07
0.8g	100	26.43	4.60	73.53
1.0g	100	34.99	3.25	65.01
<b>Dose/Pb<sup>2+</sup></b>	<b>Co mg/l (Pb<sup>2+</sup>)</b>	<b>Ce mg/l</b>	<b>q<sub>e</sub></b>	<b>%Re</b>
0.2g	100	2.5	23.45	93.80
0.4g	100	3.12	12.11	96.90
0.6g	100	6.2	8.25	99.00
0.8g	100	1	6.09	97.50
1.0g	100	2.61	4.87	97.39
<b>Dose/Zn<sup>2+</sup></b>	<b>Co mg/l (Zn<sup>2+</sup>)</b>	<b>Ce mg/l</b>	<b>q<sub>e</sub></b>	<b>%Re</b>
0.2g	100	31.55	17.11	68.45
0.4g	100	24.09	9.49	75.91
0.6g	100	13.89	7.18	86.11
0.8g	100	14.49	5.34	85.51
1.0g	100	22.57	3.87	77.43
<b>Dose/Fe<sup>2+</sup></b>	<b>Co mg/l (Fe<sup>2+</sup>)</b>	<b>Ce mg/l</b>	<b>q<sub>e</sub></b>	<b>%Re</b>
0.2g	100	0.99	24.64	98.60
0.4g	100	1.44	12.37	99.01
0.6g	100	3.71	8.27	99.18
0.8g	100	0.82	6.13	98.09
1.0g	100	1.91	4.81	96.29

**Effect of Contact Time**

The efficiency of an adsorbent in the remediation of heavy metal depends a lot on the time of adsorption. Hence, the need to study the effect of contact time in the adsorption of the heavy metals Zn<sup>2+</sup>, Pb<sup>2+</sup>, Fe<sup>2+</sup>, Cu<sup>2+</sup>.

From the result shown in Tables 1 the rate of adsorption of Cu<sup>2+</sup>, Pb<sup>2+</sup>, Zn<sup>2+</sup>, Fe<sup>2+</sup> tends to increase with increase in contact time from 20min to 30min. However, after 30min, the percentage adsorption started decreasing slowly until the time reached 50min.

This trend could be explained by the fact that a considerable number of vacant site were available for adsorption during the initial stage of the experiment and once the equilibrium time was attained, the number of

vacant site became less (Obiora and Onukwuli, 2013). Similar trends were observed by (Mustapha *et al.*, 2019) and (Ogwuche *et al.*, 2015). This indicates that the maximum adsorption was reached at 30min as further increase in time did not result in any significant change in the percentage removal of the heavy metal.

**Effect of Adsorbent Dose**

The dosage of the adsorbent used in adsorption is a very relevant parameter in the study of adsorption as it indicates the optimum dosage at which maximum removal of the heavy metal occurs. Table 4 show the percentage removal of the heavy metal at varying adsorbent doses in the dose range of 0.2g to 1.0g. The trend in adsorption shows the percentage removal

increases with increasing adsorbent dosage from 0.2g to 0.6g. This can be explained by the fact that the number of available adsorption sites as well as the surface area increase by increasing adsorbent dose and therefore, results in the increase in amount of remediated heavy metal.

However, as we move from 0.6g to 1.0g, the percentage removal decreased. This can possibly be because; the binding sites on the activated carbon get saturated through the adsorption process. This observed trend is in agreement with the results obtained for other system of adsorbent (Tan *et al.*, 2008 and Yu *et al.*, 2008).

**Table 3: Effect of pH on the remediation of heavy metals**

pH/Cu <sup>2+</sup>	Co mg/l (Cu <sup>2+</sup> )	Ce mg/l	q <sub>e</sub>	%Re
2	100	3.69	8.03	96.31
4	100	43.64	4.70	56.36
6	100	56.97	3.59	43.03
pH/Pb <sup>2+</sup>	Co mg/l (Pb <sup>2+</sup> )	Ce mg/l	q <sub>e</sub>	%Re
2	100	9.32	7.56	90.68
4	100	13.31	7.22	86.69
6	100	57.09	3.58	42.91
pH/Zn <sup>2+</sup>	Co mg/l (Zn <sup>2+</sup> )	Ce mg/l	q <sub>e</sub>	%Re
2	100	15.61	7.03	84.39
4	100	23.59	6.37	76.41
6	100	15.61	7.03	53.73
pH/Fe <sup>2+</sup>	Co mg/l (Fe <sup>2+</sup> )	Ce mg/l	q <sub>e</sub>	%Re
2	100	0.86	8.26	99.14
4	100	2.24	8.15	97.76
6	100	3.09	8.08	96.91

**Table 4: Effect of temperature on the remediation of heavy metals**

TEMP°C/Cu <sup>2+</sup>	Co mg/l (Cu <sup>2+</sup> )	Ce mg/l	q <sub>e</sub>	%Re
40	100	30.7	5.78	69.29
50	100	14.8	7.10	85.19
60	100	7.45	7.71	92.55
TEMP°C/Pb <sup>2+</sup>	Co mg/l (Pb <sup>2+</sup> )	Ce mg/l	q <sub>e</sub>	%Re
40	100	71.3	2.39	28.7
50	100	62.33	3.14	37.67
60	100	41.09	4.91	58.91
TEMP°C/Zn <sup>2+</sup>	Co mg/l (Zn <sup>2+</sup> )	Ce mg/l	q <sub>e</sub>	%Re
40	100	7.39	7.72	92.61
50	100	5.18	7.91	94.83
60	100	3.02	8.08	96.98
TEMP°C/Fe <sup>2+</sup>	Co mg/l (Fe <sup>2+</sup> )	Ce mg/l	q <sub>e</sub>	%Re
40	100	39.22	5.07	60.78
50	100	24.54	6.29	75.46
60	100	39.22	5.07	82.34

**Table 5: Effect of concentration on the remediation of heavy metal**

Co mg/l (Cu <sup>2+</sup> )	Ce mg/l	q <sub>e</sub>	%Re
20	12.08	0.66	39.58
40	25.2	1.23	58.00
60	14.02	3.83	64.95
Co mg/l (Pb <sup>2+</sup> )	Ce mg/l	q <sub>e</sub>	%Re
20	16.82	0.27	15.88
40	14.46	2.13	75.90
60	8.81	4.27	77.98
Co mg/l (Zn <sup>2+</sup> )	Ce mg/l	q <sub>e</sub>	%Re
20	7.42	1.05	62.90
40	14.49	2.13	63.48
60	13.01	3.92	75.85



Co mg/l (Fe <sup>2+</sup> )	Ce mg/l	q <sub>e</sub>	%Re
20	12.26	0.65	38.69
40	36.82	0.27	38.63
60	22.21	3.15	44.48

### Effect of pH

The degree of ionization of the sorbent and the surface charge of the adsorbent during the adsorption process is an important parameter in adsorption which is determined using pH. Tables 4 show the percentage removal of the heavy metal. It was observed that the remediation of the heavy metals decreases as the pH increases.

As the pH of the heavy metal solution increases from 2 to 6, a resulting decrease in the percentage removal of the heavy metal was observed. The trend observed can be explained by the possibility that at low pH, the surface of the adsorbent would be surrounded by hydronium ions, which might enhance the interaction of the heavy metals with the binding sites of the adsorbent by greater attractive force and hence improved its uptake on adsorbent (Memon *et al.*, 2008). Conversely, a reduced adsorption percentage was observed at higher pH which can be credited to increase in OH<sup>-</sup> leading to the formation of aqua-complexes thereby retarding the adsorption (Tiwari and Kathane, 2013). At higher pH values, the degree of dissociation of the group at the adsorbent surface is high and both the adsorbent and solutes occur in their negatively charged forms. The adsorption is consequently not favored due to the presence of some electrostatic repulsion, between the molecules and the surface adsorbent (Tiwari and Bind, 2014).

### Effect of Temperature

Table 5 show the effect of temperature on the remediation of heavy metal by the adsorbent. It was observed that the amount of heavy metal removed increases as the temperature increases suggesting that the adsorption was endothermic in nature. As the temperature increases, a considerable progressive increase was observed. This behavior could be attributed to better interaction between the adsorbent, creation of new adsorption sites and increased intra-particle diffusion at higher temperatures. This observed trend is in agreement with the results obtained and observed as a trend for the adsorption of metal ions by (Mustapha *et al.*, 2019).

### Effect of Initial Concentration

The percentage of heavy metal removed was shown on Tables 5. It was observed as a trend that the percentage heavy metal remediated increased as the concentration of the heavy metal solution is increased. The increase in concentration of heavy metal solution allows it to overcome the resistance to the mass transfer of the heavy metal between the aqueous and solid phase which also improved the interaction between the heavy metal solution and the adsorbent (Chang *et al.*, 2011). Other researchers (Tiwari and Bind, 2014) observed similar trends in the adsorption of dichlorvos.

### Adsorption Isotherm Studies

Table 6: Showing the adsorption isotherm parameters and values

Cu <sup>2+</sup>	Co(mg/l)	C <sub>e</sub> (mg/l)	1/C <sub>e</sub>	logC <sub>e</sub>	lnC <sub>e</sub>	q <sub>e</sub> (mg/g)	1/q <sub>e</sub>	logq <sub>e</sub>	
	20	6.08	0.16	0.78	1.81	1.16	0.86	0.06	
	40	11.02	0.09	1.04	2.39	2.42	0.41	0.38	
	60	14.2	0.07	1.15	2.65	3.82	0.26	0.58	
Fe <sup>2+</sup>	Co(mg/l)	C <sub>e</sub> (mg/l)	1/C <sub>e</sub>	logC <sub>e</sub>	lnC <sub>e</sub>	q <sub>e</sub> (mg/g)	1/q <sub>e</sub>	logq <sub>e</sub>	
	20	7.12	0.14	0.85	1.96	1.07	0.93	0.03	
	40	12.89	0.08	1.11	2.56	2.26	0.44	0.35	
	60	13.92	0.07	1.14	2.63	3.84	0.26	0.58	
Pb <sup>2+</sup>	Co(mg/l)	C <sub>e</sub> (mg/l)	1/C <sub>e</sub>	logC <sub>e</sub>	lnC <sub>e</sub>	q <sub>e</sub> (mg/g)	1/q <sub>e</sub>	logq <sub>e</sub>	
	20	5.2	0.19	0.72	1.65	1.23	0.81	0.09	
	40	9.62	0.10	0.98	2.26	2.53	0.39	0.40	
	60	11.33	0.09	1.05	2.43	4.06	0.25	0.61	
Zn <sup>2+</sup>	Co(mg/l)	C <sub>e</sub> (mg/l)	1/C <sub>e</sub>	logC <sub>e</sub>	lnC <sub>e</sub>	q <sub>e</sub> (mg/g)	1/q <sub>e</sub>	logq <sub>e</sub>	
	20	7.42	0.13	0.87	2.00	1.05	0.95	0.02	
	40	13.01	0.08	1.11	2.57	2.25	0.44	0.35	
	60	14.49	0.07	1.16	2.67	3.79	0.26	0.58	
Lagmuir Isotherm			Freundlich Isotherm			Temkin Isotherm			
Metal	q <sub>max</sub>	K <sub>L</sub>	R <sup>2</sup>	1/n	K <sub>f</sub>	R <sup>2</sup>	B <sub>T</sub>	K <sub>T</sub>	R <sup>2</sup>
Cu <sup>2+</sup>	5.01	0.03	0.99	1.42	2.92	0.99	3.01	0.23	0.88
Fe <sup>2+</sup>	3.09	0.04	0.93	1.66	4.04	0.80	3.32	0.19	0.54
Pb <sup>2+</sup>	5.50	0.04	0.97	1.43	2.58	0.92	3.22	0.27	0.74
Zn <sup>2+</sup>	2.73	0.04	0.96	1.73	4.48	0.86	3.45	0.18	0.63

### Adsorption Isotherm

The interaction of solute with the adsorbent is described by adsorption isotherm. The  $R^2$  value correlation coefficient was used to judge the applicability of the isotherm models for this adsorption study.

### Freundlich adsorption isotherm

An effective relationship that describes the adsorption of a solute from a liquid to the surface of a solid is the Freundlich adsorption isotherm, and is used for describing the adsorption characteristics for the heterogeneous surface (Thouria *et al.*, 2017). It is a relationship between the amount of heavy metal adsorbed by the adsorbent per unit mass of the adsorbent material ( $q_e$ ) and the concentration of the heavy metal solution at equilibrium ( $C_e$ ).

The constant  $K_f$  is an indicator of the adsorption capacity of an adsorbent, whereas,  $1/n$  shows the function of the strength of adsorption in the adsorption process (Voudrias *et al.*, 2002). If the value of  $n=1$ , the partition between the liquid and solid phases are independent of the concentration of the adsorbate. If the value of  $1/n$  is less than one it suggests a normal adsorption. On the other hand,  $1/n$  being greater than one indicates cooperative adsorption (Mohan and Karthikeyan 1997).

The  $K_f$  and  $n$  are parameters of the adsorbent-adsorbate system, which has to be determined by data fitting and linear regression is generally employed in determining the parameters of kinetic and isotherm model (Guadalupe *et al.*, 2008). The linear least-squares method and the linearly transformed equations have been widely applied to correlate sorption data where  $1/n$  is a heterogeneity parameter, the smaller  $1/n$ , the greater the expected heterogeneity. This expression reduces to a linear adsorption isotherm when  $1/n = 1$ . If  $n$  lies between one and ten, this indicates a favorable sorption process (Goldberg 2005). From the data in Table 7, that value of  $1/n$  for the heavy metals  $Cu^{2+}$ ,  $Fe^{2+}$ ,  $Pb^{2+}$  and  $Zn^{2+}$  is 1.42, 1.66, 1.43 and 1.73 while  $n$  for the heavy metals  $Cu^{2+}$ ,  $Fe^{2+}$ ,  $Pb^{2+}$  and  $Zn^{2+}$  is 0.705, 0.602, 0.669 and 0.577 indicating that the sorption of the heavy metals onto the activated carbon is not favourable and the  $R^2$  value for the heavy metals  $Cu^{2+}$ ,  $Fe^{2+}$ ,  $Pb^{2+}$  and  $Zn^{2+}$  is 0.986, 0.801, 0.918 and 0.863.

### Langmuir adsorption isotherm

The Langmuir isotherm model assumes that the adsorption of the adsorbate occurs uniformly at the active sites of the activated carbon and once an adsorbent fully takes up a site, no further adsorption of the adsorbate can take place at that occupied site.

$q_e$  = the amount of metal adsorbed per gram of the adsorbent at equilibrium (mg/g).

$q_{max}$  = maximum monolayer coverage capacity (mg/g)

$K_L$  = Langmuir isotherm constant (L/mg).

The essential features of the Langmuir isotherm is usually expressed in terms of equilibrium parameter ( $R_L$ ), a dimensionless constant known as the equilibrium parameter.

$$R_L = \frac{1}{(1 + K_L C_o)} \quad (1)$$

Where:  $C_o$  = initial concentration  $K_L$  (Langmuir Constant) = the constant that is related to the energy of adsorption. The values of  $R_L$  suggests whether the adsorption is irreversible ( $R_L = 0$ ), favourable ( $0 < R_L < 1$ ) or linear or unfavourable ( $R_L = 1$  or  $R_L > 1$ ).

For this adsorption research work,  $q_{max}$  (the maximum monolayer coverage capacity) from Langmuir Isotherm model for the heavy metals  $Cu^{2+}$ ,  $Fe^{2+}$ ,  $Pb^{2+}$  and  $Zn^{2+}$  was determined to be 5.006 mg/g, 3.088 mg/g, 5.497 mg/g and 2.729 mg/g  $K_L$  (Langmuir isotherm constant) for the heavy metals  $Cu^{2+}$ ,  $Fe^{2+}$ ,  $Pb^{2+}$  and  $Zn^{2+}$  is 0.030 L/mg, 0.036 L/mg, 0.035 L/mg and 0.037 L/mg  $R_L$  (the separation factor) for the heavy metals  $Cu^{2+}$ ,  $Fe^{2+}$ ,  $Pb^{2+}$  and  $Zn^{2+}$  is 0.36, 0.32, 0.32 and 0.31 indicating that the equilibrium sorption was favourable and the  $R^2$  value for the heavy metals  $Cu^{2+}$ ,  $Fe^{2+}$ ,  $Pb^{2+}$  and  $Zn^{2+}$  is 0.99, 0.93, 0.97 and 0.96 proving that the sorption data fitted well to Langmuir Isotherm model. The results are in agreement with the work of (Mustapha *et al.*, 2019).

### Temkin isotherm

This isotherm contains a factor that clearly takes into account the interaction of the adsorbent-adsorbate. The isotherm is based on the assumption that due to the repulsions between adsorbent-adsorbate the heat of adsorption decreases linearly as the coverage of molecules and the adsorption of adsorbate is uniformly distributed. (Temkin and Pyzhev, 1940).

The Temkin isotherm data are also shown in Table 4.7. The values of correlation coefficient,  $R^2$  value for the heavy metals  $Cu^{2+}$ ,  $Fe^{2+}$ ,  $Pb^{2+}$  and  $Zn^{2+}$  is 0.88, 0.54, 0.74 and 0.63. and  $K_T$  value for the heavy metals  $Cu^{2+}$ ,  $Fe^{2+}$ ,  $Pb^{2+}$  and  $Zn^{2+}$  adsorption is estimated to be 0.23, 0.19, 0.27 and 0.18 respectively. The poor correlation coefficient,  $R^2$ , for heavy metal indicates that the model does not fit into the data. From the tables 7, it is clear that Langmuir adsorption isotherm is the most favoured in the adsorption process with the value of the correlation coefficient obtained from the three models for all the four heavy metals ( $R^2 \geq 0.9$ ).

**Table 7: Showing the adsorption thermodynamics**

(Cu <sup>2+</sup> )/T(°C)	T(KELVIN)	1/T	C <sub>0</sub> (mg/l)	C <sub>e</sub> (mg/l)	q <sub>e</sub>	K <sub>L</sub>	lnK <sub>L</sub>	R
40	313	0.003195	60	4.51	4.62	1.02	0.02	8.314
50	323	0.003096	60	3.82	4.68	1.23	0.21	8.314
60	333	0.003003	60	2.63	4.78	1.82	0.59	8.314
<b>ΔG°K J/mol</b>	<b>Intercept</b>	<b>Slope</b>	<b>R<sup>2</sup></b>	<b>ΔH°KJ/mol</b>	<b>ΔS°(J/mol/K)</b>			
<b>-0.05</b>	9.59	-3005.64	0.91	24.99	79.70			
<b>-0.56</b>								
<b>-1.66</b>								
(Fe <sup>2+</sup> )/T(°C)	T(K)	1/T	C <sub>0</sub> (mg/l)	C <sub>e</sub> (mg/l)	q <sub>e</sub>	K <sub>L</sub>	lnK <sub>L</sub>	R
40	313	0.003195	60	4.46	4.63	1.04	0.04	8.314
50	323	0.003096	60	3.76	4.69	1.25	0.22	8.314
60	333	0.003003	60	2.58	4.79	1.86	0.62	8.314
<b>ΔG°K J/mol</b>	<b>Intercept</b>	<b>Slope</b>	<b>R<sup>2</sup></b>	<b>ΔH°(KJ/mol)</b>	<b>ΔS°(J/mol/K)</b>			
-0.10	9.64	-3017.26	0.91	25.09	80.16			
-0.59								
-1.72								
(Pb <sup>2+</sup> )	T(KELVIN)	1/T	C <sub>0</sub> (mg/l)	C <sub>e</sub> (mg/l)	q <sub>e</sub>	K <sub>L</sub>	lnK <sub>L</sub>	R
40	313	0.003195	60	4.35	4.64	1.06	0.06	8.314
50	323	0.003096	60	3.55	4.70	1.32	0.28	8.314
60	333	0.003003	60	2.56	4.79	1.87	0.63	8.314
<b>ΔG°K J/mol</b>	<b>Intercept</b>	<b>Slope</b>	<b>R<sup>2</sup></b>	<b>ΔH°(KJ/mol)</b>	<b>ΔS°(J/mol/K)</b>			
-0.15	9.46	-2950.5	0.96	24.53	78.66			
-0.75								
-1.73								
(Zn <sup>2+</sup> )	T(KELVIN)	1/T	C <sub>0</sub>	C <sub>e</sub>	q <sub>e</sub>	K <sub>L</sub>	lnK <sub>L</sub>	R
40	313	0.003195	60	4.53	4.63	1.02	0.02	8.314
50	323	0.003096	60	3.74	4.69	1.25	0.22	8.314
60	333	0.003003	60	2.62	4.78	1.82	0.59	8.314
<b>ΔG°K J/mol</b>	<b>Intercept</b>	<b>Slope</b>	<b>R<sup>2</sup></b>	<b>ΔH°(KJ/mol)</b>	<b>ΔS°(J/mol/K)</b>			
-0.052	9.59	-3007.38	0.93	25.00	79.79			
-0.59								
-1.66								

### Thermodynamics Study

By computing the amount of heavy metals adsorbed at various time of adsorption, the rate constant  $k_L$  was determined at each temperature values of 40°C, 50°C and 60°C. The thermodynamic study was carried out at various temperature values, exploring other thermodynamic parameters such as  $\Delta G^\circ$ =Gibb-free energy,  $\Delta H^\circ$ =Enthalpy and  $\Delta S^\circ$ =Entropy of adsorption. Enthalpy was gotten from the slope of the plot of  $1/T$  against  $\ln k_L$  as shown in the graphs while the values of  $\Delta S^\circ$  and  $\Delta G^\circ$  were calculated using the equations;

$$\Delta G^\circ = -RT \ln k_L \quad (2)$$

$$\Delta G = \Delta H - T\Delta S \quad (3)$$

$$-RT \ln k_L = \Delta H - T\Delta S \quad (4)$$

$$\ln k_L = -\frac{\Delta H}{RT} + \frac{\Delta S}{R} \quad (5)$$

$$\Delta S^\circ = \frac{\Delta H - \Delta G}{T} \quad (6)$$

The positive values of enthalpy ( $\Delta H$ ) indicate that the adsorption process was endothermic in nature, while the positive values of  $\Delta S$  expresses the affinity of the adsorbent for the heavy metal ions in the adsorbate, indicating an increase in adsorbate concentration in the adsorbent-adsorbate interface. The thermodynamic parameters show that the adsorption of metal ions is non-spontaneous at low temperature, while spontaneity occurs at high-temperature values. The adsorption of the heavy metal is spontaneous at the temperatures under investigation as seen by the negative values of free energy ( $\Delta G$ ). Similar results was reported on different types of adsorbent in the research by (Ahmed *et al.*, 2015).

**Table 8: Showing the adsorption kinetics**

$\text{Cu}^{2+}$	Time(min)	$C_i(\text{mg/l})$	$C_e(\text{mg/l})$	$q_e(\text{mg/g})$	$q_t(\text{mg/g})$	$(q_e - q_t)$	$\ln(q_e - q_t)$	$t/q_t$
	20	60	48.72	3.83	0.94	2.89	1.06	21.28
	30	60	34.17	3.83	2.15	1.68	0.52	13.94
	40	60	35.34	3.83	2.06	1.78	0.57	19.46
	50	60	34.91	3.83	2.09	1.74	0.55	23.91
	60	60	36.11	3.83	1.99	1.84	0.61	30.14
$\text{Pb}^{2+}$	Time(min)	$C_i(\text{mg/l})$	$C_e(\text{mg/l})$	$q_e(\text{mg/g})$	$q_t(\text{mg/g})$	$(q_e - q_t)$	$\ln(q_e - q_t)$	$t/q_t$
	20	60	44.03	4.27	1.33	2.94	1.08	15.03
	30	60	31.67	4.27	2.36	1.91	0.65	12.71
	40	60	32.18	4.27	2.32	1.95	0.67	17.25
	50	60	38.59	4.27	1.78	2.49	0.91	28.02
	60	60	32.15	4.27	2.32	1.95	0.67	25.85
$\text{Zn}^{2+}$	Time(min)	$C_i(\text{mg/l})$	$C_e(\text{mg/l})$	$q_e(\text{mg/g})$	$q_t(\text{mg/g})$	$(q_e - q_t)$	$\ln(q_e - q_t)$	$t/q_t$
	20	60	47.15	3.92	1.07	2.85	1.05	18.68
	30	60	30.25	3.92	2.48	1.44	0.37	12.10
	40	60	32.02	3.92	2.33	1.59	0.46	17.16
	50	60	34.71	3.92	2.11	1.81	0.59	23.72
	60	60	35.64	3.92	2.03	1.89	0.64	29.56
$\text{Fe}^{2+}$	Time(min)	$C_i(\text{mg/l})$	$C_e(\text{mg/l})$	$q_e(\text{mg/g})$	$q_t(\text{mg/g})$	$(q_e - q_t)$	$\ln(q_e - q_t)$	$t/q_t$
	20	60	45.72	3.15	1.19	1.96	0.67	16.81
	30	60	36.13	3.15	1.99	1.16	0.15	15.08
	40	60	38.71	3.15	1.77	1.38	0.32	22.55
	50	60	37.67	3.15	1.86	1.29	0.25	26.87
	60	60	39.01	3.15	1.75	1.40	0.34	34.30

**Table 9a: Parameters of pseudo-first-order kinetic model for heavy metal adsorption**

Pseudo-First-Order Model						
Heavy Metals	Intercept	Slope	$q_e(\text{mg/g})$	$k_1$	$R^2$	$q_e(\text{exp})$
$\text{Cu}^{2+}$	1.01013	-0.01	2.745958	-0.000145	0.1621	3.83
$\text{Pb}^{2+}$	1.0173	-0.01	2.765717	-0.000093	0.21035	4.27
$\text{Fe}^{2+}$	0.85781	-0.006	2.357991	-0.000099	0.12816	3.92
$\text{Zn}^{2+}$	0.5732	-0.006	1.773935	-0.000095	0.20745	3.15

**Table 9b: Parameters of pseudo-second-order kinetic model for heavy metal adsorption**

Pseudo-Second-Order Model						
Heavy Metals	Intercept	Slope	$q_e(\text{mg/g})$	$k_2$	$R^2$	$q_e(\text{exp})$
$\text{Cu}^{2+}$	10.66625	0.277	3.610108	0.007194	0.38951	3.83
$\text{Pb}^{2+}$	4.98683	0.26966	3.708374	0.014582	0.65779	4.27
$\text{Fe}^{2+}$	6.88962	0.33383	2.995537	0.016175	0.50546	3.92
$\text{Zn}^{2+}$	4.40973	0.46779	2.137711	0.049624	0.32511	3.15

### Kinetic Adsorption Study

In order to investigate the mechanism of adsorption of heavy metals, pseudo-first-order and pseudo-second-order kinetics models were employed to the equilibrium data obtained from the effect of contact time. Table 9 shows the comparison between the values of the  $q_e$  (adsorption rate constant) and  $R^2$  (correlation coefficient) linked to the pseudo-first-order and pseudo-second-order adsorption of the heavy metals.

The value for the experimental adsorption capacity for  $\text{Cu}^{2+}$ ,  $\text{Pb}^{2+}$ ,  $\text{Fe}^{2+}$  and  $\text{Zn}^{2+}$  are 3.83, 4.27, 3.92 and 3.15 respectively. From the table 5.0a and 5.0b, it can be seen that, the corresponding calculated adsorption capacity for

the pseudo-second-order model for the heavy metals  $\text{Cu}^{2+}$ ,  $\text{Pb}^{2+}$ ,  $\text{Fe}^{2+}$  and  $\text{Zn}^{2+}$  were closer to the experimental adsorption capacity than the calculated adsorption capacity for the pseudo-first-order model.

The correlation coefficient,  $R^2$  values for the pseudo-second-order adsorption model are higher than that of the pseudo-first-order adsorption model, which suggest that the adsorption is dependent on the initial concentration. This concludes that, the pseudo-second-order adsorption is best suited in describing the adsorption kinetics of the heavy metals on the *Hyphaene thebaica*. The pseudo-second-order model relies on the assumption that adsorption may be the rate limiting step (Gupta and

Rastogi, 2009). Therefore, the rate limiting step for this study is an indication of chemisorption.

## CONCLUSION

The activated carbon was imaged by means of scanning electron microscope. The images taken at the magnifications of 5000x and 7000x showed that micropores were visible as a result of the physiochemical treatment thus increasing the surface area. The FTIR spectroscopic technique was employed in identifying the various functional groups present on the activated carbon, showed that the spectrum of activated carbon, showed that, the spectrum of activated carbon after adsorption of the heavy metals was characterized by shifts in the position and intensities of bands when compared to the spectrum of the activated carbon before adsorption, indicating that interaction were established during the remediation of the heavy metal. The optimization studies showed maximum adsorption at the following conditions: contact time (30min), adsorbent dose (0.6g), pH (2), temperature (60°C) and adsorbate concentration (60mg/l). The Lagmuir, Freundlich and Temkin isotherm model were tested and Lagmuir isotherm model was found to be most fitted for the adsorption process with the value of the correlation coefficient obtained from the four heavy metals being greater than or equal to 0.9. The kinetic of adsorption study was tested with pseudo-first-order and pseudo-second-order models. The correlation coefficient  $R^2$  value for the pseudo-second-order adsorption model was higher than that of the pseudo-first-order which implies that pseudo-second-order is more favoured. Thermodynamic parameters ( $\Delta G^\circ$ ,  $\Delta H^\circ$  and  $\Delta S^\circ$ ) obtained at various temperature were positive for  $\Delta H^\circ$  and  $\Delta S$  which indicates that the adsorption was endothermic and expresses the affinity of the adsorbent for the heavy metal ions in the adsorbate. The negative values of the  $\Delta G^\circ$  indicated that the adsorption of heavy metal is spontaneous at the temperature under investigation.

## REFERENCES

Abbas, A. F, Ahmed MJ (2016) Mesoporous activated carbon from date stones (*Phoenix dactyliferous* L.) by one-step microwave assisted  $K_2CO_3$  pyrolysis. *J Water Process Eng* 9:201–207.

Abel A. A., Mellisa Uzoukwu C., Popoola L.T., Yusuff A.S., Bernard E., Pam A.A., Ogunyemi A.T., Hamisu A. (2022) Equilibrium and Kinetic Analysis on Cadmium Ion Sequestration from Aqueous Environment by Impregnated Chicken Feather Alkaline Biosorbent *International Journal of Engineering Research in Africa*, Vol. 60, pp 15-28

Adeyemo A.A., Adeoye I.O. and Bello O.S., (2015) Adsorption of dyes using different types of clay: a review, *Appl. Water Sci.*

Adinata D, Daud W. M, Aroua, M. K (2007) Preparation and characterization of activated carbon from palm shell by chemical activation with  $K_2CO_3$ . *Bioresour Technol.* 98:145–149.

Ahmad M.A., Ahmad Puad N.A. and Bello O.S., (2014) Kinetics, equilibrium and thermodynamics studies of synthetic dye removal using pomegranate peel activated carbon prepared by microwave-induced KOH activation, *Water Resc. Ind.*, 6, 18-35

Ahmad Mohd Azmier, Norhidayah Ahmad & Olugbenga Solomon Bello (2015) Adsorption Kinetic Studies for the Removal of Synthetic Dye Using Durian Seed Activated Carbon, *Journal of Dispersion Science and Technology*, 36:5, 670-684, doi: 10.1080/01932691.2014.913983

Alexandra Semenova, Luke w. (2022) giles, mark Louis p. vidallon, bart follink, paull, brown rico f. tabor. Copper-binding properties of polyethylenimine-silica nanocomposite particles. *Lagmuir*, 38(34), 10585-10600.

Allen, and Koumanova (2005), Decolourisation of water/wastewater using adsorption (review), *J. University Chem. Technol. Metallurgy*, 40(3), 175-192

Amin N.K., (2008) Removal of reactive dye from aqueous solutions by adsorption onto activated carbons prepared from sugarcane bagasse pith, *Desalination*, 223, 152-161

Anthony Staden (1970). *Kirk-Othmer Encyclopedia*, vol. 4, 2nd ed., McGraw-Hill, New York, USA.

Aremu, A. K. and Fadele, O. K. (2011). Study of some properties of doum palm fruit (*Hyphaenethebaica* Mart.) in relation to moisture content. *African Journal of Agricultural Research*, 6(15): 3597-3602

Asia, O., Ndubuisi, L., and Odia, A. (2009). Studies on the pollution potential of wastewater from textile processing factories in Kaduna, Nigeria. *Journal of Toxicology and Environmental Health Sciences*, 1 (2):034-037

Autu, M. and Hameed, B.H. (2011) Optimized waste Tea Activated Carbon for Adsorption of Methylene Blue and Acid Blue 29 Dyes using Response Surface Methodology. *Chemical Engineering Journal*, 175: 233–243

- Bakatula, EliseeNsimba; Richard, Dominique; Neculita, Carmen Mihaela; Zagury, Gerald J. (2018)."Determination of point of zero charge of natural organic materials".Environmental Science and Pollution Research. 25 (8): 7823–7833
- Balajii M, Niju S (2019) Biochar-derived heterogeneous catalysts for biodiesel production. Environ ChemLett. <https://doi.org/10.1007/s10311-019-00885-x>
- Bedin KC, Martins AC, Cazetta AL (2016) KOH-activated carbon prepared from sucrose spherical carbon: adsorption equilibrium, kinetic and thermodynamic studies for Methylene Blue removal. ChemEng J 286:476–484. <https://doi.org/10.1016/j.cej.2015.10.099>
- Bergna D., Hu T., Prokkola H., Romar H., Lassi U., (2019) Effect of some process parameters on the main properties of activated carbon produced from peat in a Lab-scale Process. Waste and biomass valorization 11:2837-2848
- Bernard E., Jimoh A. and Odigure J.(2013). Heavy Metals Removal from Industrial Wastewater by Activated Carbon Prepared from Coconut Shell, *Research Journal of Chemical Sciences* 3(8):3-9
- Bharathi K.S. and RameshS.T., Removal of dyes using agricultural waste as low-cost adsorbents: a review, Appl. Water Sci.,3, 773-790 (2013)
- Bhatnagar A, Hogland W, Marques M, Sillanpää M (2013) An overview of the modification methods of activated carbon for its water treatment applications. ChemEng J 219:499–511.
- Boehm, H.P. (1994)Some aspects of the surface chemistry of carbon blacks and other carbons. J. Carbon, 32,759–769.
- Bouchelta C, Medjram MS, Bertrand O, Bellat J-P (2008) Preparation and characterization of activated carbon from date stones by physical activation with steam. J Anal Appl Pyrolysis 82:70–77.
- BrahimI.,Ould, BelmedaniM., BelgacemA., HadounH. andSadaouiZ., (2014) Discoloration of azodye solutions by adsorption on activated carbon prepared from the cryogenic grinding of used tires, Chem. Eng. Transactions, 38, 121-126
- Budinova T, Petrov N, Parra J, Baloutzov V (2008) Use of an activated carbon from antibiotic waste for the removal of Hg(II) from aqueous solution. J Environ Manage 8:165–172.
- Byamba-Ochir N, Shim WG, Balathanigaimani M, Moon H (2016) Highly porous activated carbons prepared from carbon rich Mongolian anthracite by direct NaOH activation. Appl Surf Sci 379:331–337.
- Chada, Nagaraju&Romanos, jimmy & Hilton, ramsey&suppes, galen&burrell, Jacob &pfeifer, peter. (2012). Activated carbon monoliths for methane storage. 33012
- DasN. and CharumathiD.(2012), Remediation of synthetic dyes from wastewater using yeast – An overview, Indian J. Biotech.,11, 369-380
- Demirbas A., Agricultural based activated carbons for the removal of dyes from aqueous solutions: a review, J. Hazard. Mater.,167, 1-9 (2009)
- Ekpete O. A., Kpee F., Amadi J. C. and Rotimi R. B., Adsorption of Chromium (VI) and Zinc (II) Ions on the Skin of Orange Peels, J. of Nep Chem Soc., (26), 32-38 (2010)
- El-SayedG.O., YehiaM.M. and AsaadA.A., (2014)Assessment of activated carbon prepared from corncob by chemical activation with phosphoric acid, Water Resc. Ind.,7-8, 66-75
- Ernst, W.R. (1979). Adsorption of textile dyes from aqueous solution by activated carbon from peanut hulls. Georgia Institute of Technology, USA.
- EtimU.J., UmorenS.A. and EduokU.M.,(2012) Coconut coir dust as a low cost adsorbent for the removal of cationic dye from aqueous solution, J. Saudi Chem. Society.
- Foo K, Hameed B (2012c) Preparation, characterization and evaluation of adsorptive properties of orange peel based activated carbon via microwave induced K<sub>2</sub>CO<sub>3</sub> activation. *Bioresour Technol.*104:679–686.
- Franca, A. S., Oliveira, L. S., and Ferreira, M. E. (2009).Kinetics and Equilibrium Studies of Methylene Blue Adsorption by Spent Coffee Grounds. Desalination, 249-267.
- Garg, V.K., Gupta, R., Yadav, A.B., Kumar, R. (2003): Dye removal from aqueous solution by adsorption on treated sawdust. *Bioresources. Technol.*, 89, pp 121-124.
- GhaediM., TavallaliH., SharifiM., Kokhdan S.N., andAsghariA., (2012) Preparation of low cost activated carbon from MyrtusCommunis and pomegranate and their efficient application for removal of congo red from

- aqueous solution, *SpectrochimicaActa Part A*,86, 107-114
- Goldberg, S. (2005). Equations and Models Describing Adsorption Processes in Soils. In *Chemical Processes in Soils* (No. 8, pp.489-517). Madison, WI: Soil Science Society of America.
- Gopinath A, Kadirvelu K (2018) Strategies to design modified activated carbon fibers for the decontamination of water and air. *Environ ChemLett* 16:1137–1168.
- Griffiths, P.; de Hasseth, J. A. (2007). *Fourier Transform Infrared Spectrometry* (2nd ed.). Wiley-Blackwell. ISBN 978-0-471-19404-0.
- Guadalupe R., Reynel-Avila H.E, Bonilla-Petriciolet A., Cano-Rodríguez I., Velasco-Santos C., and Martínez-Hernández A.L.(2008). Recycling poultry feathers for Pb removal from wastewater: kinetic and equilibrium studies. *Proceedings of World Academy of Science, Engineering and Technology Volume 30*.
- Guo, J. and Lua, C.A. (2003). Preparation and characterization of chars from oil palm waste. *Carbon*, 36, pp 1663-167.
- Gupta, V.K., and Rastogi, A. (2007). Biosorption of Lead from Aqueous Solutions by Green Algae *Spirogyra* Species: Kinetics and Equilibrium Studies. *J Colloid Interface Sci.*, 296, 59 – 63.
- Hameed BH, Din ATM, Ahmad A L.(2007) "Adsorption of Methylene Blue onto BambooBased Activated Carbon: Kinetics and Equilibrium Studies," *Journal of Hazardous Materials.*;141(3):819-825.
- Hanna, F., Jan K. and Kułazyński, M.(2015). Preparation and characterization of activated carbons from biomass material – giant knotweed (*Reynoutriasachalinensis*). *Open Chem.*, 13: 1150–1156
- HazzaaR. and HusseinM.,(2015) Adsorption of cationic dye from aqueous solution onto activated carbon prepared from olive stones, *Environ. Technol. Innovation*,4, 36-51
- HeibatiB., Rodriguez-CoutoS., Al-GhoutiM.A., AsifM., TyagiI., AgarwalS. and GuptaV.K.,(2015) Kinetics and thermodynamics of enhanced adsorption of the dye AR 18 using activated carbons prepared from walnut and poplar woods, *J. Molecular Liquid*,208, 99-105
- HidayatD.N., Maming, S. Liong, (2017) Utilization of chicken feather biomass as metal zinc adsorbent (Zn<sup>2+</sup>), *Indonesia ChimicaActa* 10(2) 11-24.
- Horikawa T, Kitakaze Y, Sekida T (2010) Characteristics and humidity control capacity of activated carbon from bamboo. *BioresourTechnol* 101:3964–3969.
- Hsu B, Coupur IM, Ng K (2006). Antioxidant Activity of Hot Water Extract from the Fruit of the Doum Palm, *Hyphaenethebaica*. *Food Chem.*, Elsevier Science Direct. 98: 317–328.
- Huang F-C, Lee C-K, Han Y-L (2014) Preparation of activated carbon using micro-nano carbon spheres through chemical activation. *J Taiwan InstChemEng* 45:2805–2812. <https://doi.org/10.1016/j.jtice.2014.08.004>
- Jain K.K., Guru P. and Singh V.,(1979) *J. of ChemTechnol Biotech.*, 29, 36–38
- Kalderis, D. (2008). Production of activated carbon from bagasse and rice husk by a single-stage chemical activation method at low retention times. *Bioresource technology*. 99(15): p. 6809-6816
- Kaneko, K.; Ishii, C.; Ruike, M.; Kuwabara, H. (1992). "Origin of superhigh surface area and microcrystalline graphitic structures of activated carbons". *Carbon*. 30 (7): 1075–1088.
- Kosheleva RI, Mitropoulos AC, Kyzas GZ (2019) Synthesis of activated carbon from food waste. *Environ ChemLett* 17:429–438. <https://doi.org/10.1007/s10311-018-0817-5>
- Liao S-W, Lin C-I, Wang L-H (2011) Kinetic study on lead(II) ion removal by adsorption onto peanut hull ash. *J Taiwan InstChemEng* 42:166–172
- Malik, R. Ramtek, D. and Wates, S. (2006). Physico-chemical and Surface Characterization of Adsorbents from Groundnut shell by ZnCl<sub>2</sub> Activation and its Ability to Adsorb Color. *Journal of Chemical Technology*, 13: 329-333
- ManiatisK., and Nurmala M. (1992). Activated carbon production from biomass. *Biomass Energy Ind. Environ.*, 274, 1034-1308.
- Manor, Joshua; Feldblum, Esther S.; Arkin, Isaiah T. (2012). "Environment Polarity in Proteins Mapped Noninvasively by FTIR Spectroscopy". *The Journal of Physical Chemistry Letters*. 3 (7): 939–944.
- Mattson, J.S. and Mark, H.B. (1971). *Activated carbon: Surface chemistry and adsorption from solution*, Marcel Dekker, New York.

- Miguel, G.S., Fowler, G.D., Sollars, C.J. (2003). A study of the characterization of activated carbons produced by steam and carbon dioxide activation of waste tyre rubber. *Carbon*, 41, pp 1009-1016.
- Moecher, David, (2004), Characterization and Identification of Mineral Unknowns: A Mineralogy Term Project, *Jour. Geoscience Education*, v 52 #1, p. 5-9.
- Mohanty, K., Jha, M., Meikap, B.C., Biswas, M.N. (2005). Removal of chromium (VI) from dilute aqueous solutions by activated carbon developed from Terminalia arjuna nuts activated with zinc chloride. *Chem. Eng. Sci.* 60, pp 3049-3059
- Mohan S. and Karthikeyan J. (1997), Removal of lignin and tannin color from aqueous solution by adsorption on to activated carbon solution by adsorption on to activated charcoal, *Environ. Pollut.* 97, pp.183-187
- MohdSalleh M.A., Mahmoud D. K., Awang Abu N.A., Wan Abdul Karim W.A. and Idris A., (2012) Methylene blue adsorption from aqueous solution by langsat (*lansium domesticum*) peel, *J. Purity, Utility Reaction Environ.*, 1, 472-495
- MohdSalleh M.A., Mahmoud D.K., Wan Abdul Karim W.A. and Idris A., (2011) Cationic and anionic dye adsorption by agricultural solid wastes: A comprehensive review, *Desalination*, 280, 1-13
- Mone M., Lambropoulou D.A., Bikiaris D.N., (2020) Chitosan Grafted with Biobased 5-Hydroxymethyl-Furfural as Adsorbent for Copper and Cadmium Ions Removal. *Polymers* 12 1-21.
- Moore, D. M. and R. C. Reynolds, Jr. 1997. X-Ray diffraction and the identification and analysis of clay minerals. 2nd Ed. Oxford University Press, New York.
- Morin-Crini N, Loiacono S, Placet V et al (2019) Hemp-based adsorbents for sequestration of metals: a review. *Environ Chem Lett* 17:393-408.
- Mustapha S. Shuaib D. T., Ndamitso M. M., Etsuyankpa M. B., Sumaila A., Mohammed U. M., Nasirudeen M. B. (2019) Adsorption isotherm, kinetic and thermodynamic studies for the removal of Pb(II), Cd(II), Zn(II) and Cu(II) ions from aqueous solutions using Albizia lebeck pods: *Applied Water Science* 9:142 <https://doi.org/10.1007/s13201-019-1021-x>
- Njoku V, Foo K, Asif M, Hameed B (2014) Preparation of activated carbons from rambutan (*Nephelium lappaceum*) peel by microwave-induced KOH activation for acid yellow 17 dye adsorption. *Chem Eng J* 250:198-204.
- Nowicki P, Kuszyńska I, Przepiórski J, Pietrzak R (2013) The effect of chemical activation method on properties of activated carbons obtained from pine cones. *Open Chem* 11:78-85.
- Nurmiyanto A., Adyandana J., Satrania M., Lady E.A., Artha Y.A., Andik Y., (2016) Chicken Feather Waste as Biosorbent for Chromium (VI) Removal From Aqueous Solution. *icsbe2014, Third Conference on Sustainable Built Environment* 1-11.
- Obiora-Okafo, I.A., Onukwuli, O.D. (2013). Utilization of Sawdust (*Gossweilerodendron balsamiferum*) as an Adsorbent for the Removal of Total Dissolved Solid Particles from Wastewater. *International Journal of Multidisciplinary Sciences and Engineering*, 4 (4), 45-53.
- Ogwuche E. O., Gimba C. E., Abechi E. S., (2015) An Evaluation of the Adsorptive Behaviour of Activated Carbon Derived from *Hyphaene Thebaica* Nut Shells for the Removal of Dichlorvos from Wastewater. *The International Journal Of Science & Technology (ISSN 2321 – 919X)*.
- Oluwaseun, E. O., Raimi, M. O., & Faisal, S. (2018). Assessment of Heavy Metals in Effluent Water Discharges from Textile Industry and River Water at Close Proximity: A Comparison of Two Textile Industries from Funtua and Zaria, North Western Nigeria. *Madridge Journal of Agriculture and Environmental Sciences*, 3-5.
- Omri, A., Wali, A., and Benzina, M. (2012). Adsorption of Bentazon on Activated Carbon Prepared from Lawsonia inermis Wood: Equilibrium, Kinetic and Thermodynamic studies. *Arabian Journal of Chemistry*, 1-11.
- Onyeji L. I. and Aboje A. A., (2011) Removal of Heavy Metals from Dye Effluent using activate carbon produced from Coconut Shell, *Int. J. of EngSci and Technol.*, 3(12), 8240- 8243
- Otaru, A. A. (2013). Characterization of activated carbon from Rice husk ash, 30-38.
- Ozacar, M., and Sengil, I. A., (2005). Adsorption of Metal Complex Dyes from Aqueous Solutions by Pine Saw Dust. *Bioresource Technology*, 96, 791– 795.
- Pallarés J, González-Cencerrado A, Arauzo I (2018) Production and characterization of activated carbon from barley straw by physical activation with carbon dioxide



and steam. *Biomass Bioenergy* 115:64–73.  
<https://doi.org/10.1016/j.biombioe.2018.04.015>

Richardson, J.F., Harker, J.H., Backhurst, J.R. (2002). *Particle Technology and Separation Processes*, vol. 2, 5th ed., ButterworthHeinemann

Robert Perry, H. and Don Green, w. (2003). *Perry's Chemical Engineers Handbook*, 7th., ed., McGraw-Hill Inc.

Robinson, T., Chandran, B., Nigam, P. (2002): Removal of dyes from artificial textile dye effluent by two agricultural waste residues, corncorb and barley husk. *Environ. Inter.*, 28, pp 29-33.

Ruthven, D.M. (1984). *Principles of Adsorption Processes*, Wiley, New York.

Salil, K.G., Shyamal, K.S., Siddharthar, D. (2005). *Introduction to Chemical Engineering*, Tata McGraw-Hill, New Delhi.

SaminuMurtalaYakasai, Shina Ismail Sadiq, SalisuNasir (2021) Adsorption thermodynamics of textile effluents using activated carbon made from palm kennel husk. *Dutse Journal of Pure and Applied Science* 7:2635-3490

Samsuri A, Sadegh-Zadeh F, Seh-Bardan B (2014) Characterization of biochars produced from oil palm and rice husks and their adsorption capacities for heavy metals. *Int J Environ Sci Technol* 11:967–976

Sharma Y.C. and UmaS., (2010) Optimization of parameters for adsorption of methylene blue on a low-cost activated carbon, *J. Chem. Eng. Data*,55, 435-439

Sposito, Garrison (1998). "On Points of Zero Charge". *Environmental Science & Technology*. 32 (19):2815–2819

Stokes, Debbie J. (2008). *Principles and Practice of Variable Pressure Environmental Scanning Electron Microscopy (VP-ESEM)*. Chichester: John Wiley & Sons.

Taha M Elmorsi (2011), equilibrium isotherms and kinetic studies of removal of methylene Blue Dye by Adsorption onto Miswak Leaves as a Natural Adsorbent, *Journal of environmental protection* 02(06) 5-9

TamburliniG., EhrensteinO.V., BertolliniR.,(2002) *Children's Health and Environment: A Review of Evidence*, WHO/European Environment Agency, Geneva, p. 223.

Tan I., Ahmad,L. and Hameed B.H.(2007). Preparation of activated carbon from coconut husk: Optimization study on removal of 2,4,6-trichlorophenol using response surface methodology. *Journal of Hazardous Materials* 153: 709–717

TanI.A.W., AhmadA.L. andHameedB.H., (2008) Adsorption of basic dye on high-surface-area activated carbon prepared from coconut husk: Equilibrium, kinetic and thermodynamic studies, *J. Hazard. Mater.*, 154 337–346.

Tay T, Ucar S, Karagöz S (2009) Preparation and characterization of activated carbon from waste biomass. *J Hazard Mater* 165:481–485.<https://doi.org/10.1016/j.jhazmat.2008.10.011>

Thouria,B.Ammar,S.Djaffar,D.,(2017) Adsorption of copper(II) ions from aqueous solution using bottom ash of expired drugs incineration,*J.Adsorption science and technology* 36(4)5-7

Tiwari, A., and Bind, A. (2014). Effective Removal of Pesticide (Dichlorvos) by Adsorption onto Super Paramagnetic Poly (Styrene-co-acrylic Acid) Hydrogel from Water. *International Research Journal of Environment Sciences*, 3 (11), 41-46.

Tiwari, A., and Kathane, P. (2013). Super Paramagnetic PVA-Alginate Microspheres as Adsorbent for Cu(II) ions Removal from Aqueous Systems. *Inter. Res. J. of Environ. Sci.*, 2 (7), 44-53.

Voudrias E., FytianosF. and Bozani E.:(2002) Sorption Description isotherms of Dyes from aqueous solutions and Waste Waters with Different Sorbent materials, *Global Nest, The Int.J.* 4(1),75-83

Verla, A. M.(2012). Activated carbon produced from Fluted pumpkin seed shell 123(1-2), 13-19

WHO (2003): *Shaping the Future World Health Organization*. 1211 Geneva 27, Switzerland.

WHO. (2002). *Water Pollutants: Biological Agents, Dissolved Chemicals, Non-dissolved Chemicals, Sediments*, Heat.Amman, Jordan.: WHO CEHA.

WongSyieluing, NorzitaNgadi, Ibrahim M. Inuwa, Onn Hassan (2018),Recent advances in applications of activated carbon from biowaste for wastewater treatment: *Journal of Cleaner Production*,175:361-375.

Yagmur, E., M. Ozmak, Z. Aktas,(2008) A novel method for production of activated carbon from waste tea by

- chemical activation with microwave energy, *Fuel* 87 3278–3285
- Yahya MA, Al-Qodah Z, Ngah CZ (2015) Agricultural bio-waste materials as potential sustainable precursors used for activated carbon production: a review. *Renew Sustain Energy Rev* 46:218–235.
- Yasin Y., Hussein M.Z. and Ahmad F., (2007) Adsorption of methylene blue onto treated activated carbon, *Malaysian J. Anal. Sci.* 11(11), 400-406
- Yilmaz E., Memon S. and Yilmaz M., (2010) Removal of direct azo dyes and aromatic amines from aqueous solution using two  $\beta$ -cyclodextrin-based polymers, *J. Hazard. Mater.*, 174, 592-597
- Yorgun S, Yıldız D, Şimşek YE (2016) Activated carbon from paulownia wood: yields of chemical activation stages. *Energy Sources Part A* 38:2035–2042.
- Yousef M, Arami SM, Takallo H et al (2019) Modification of pumice with HCl and NaOH enhancing its fluoride adsorption capacity: kinetic and isotherm studies. *Hum Ecol Risk Assess* 25:1508–1520.
- Yu, L. J., Shukla, S. S., Dorris, K. L., Shukla, A., and Margrove, J. L. (2003). Adsorption of Chromium from Aqueous Solutions by Maple Sawdust. *Journal of Hazardous Materials*, 100 (1-3), 53–63.
- Yusuff RO, Sonibare JA (2004). Characterization of Textile Industries Effluents in Kaduna, Nigeria and Pollution Implications. *Global Nest: The Int. J.* 6 (3): 212-221
- Zhang D., Yang H., Chen Y., Ran M. and Gu J. (2017), Study on the application of KOH to produce activated carbon to realize the utilization of distiller's grains. *IOP Conf. Series: Earth and Environmental Science* 69(1):20-51